Available online at www.sciencedirect.com

ScienceDirect

Energy Procedia 136 (2017) 349–355

Energy Procedia

www.elsevier.com/locate/procedia

4th International Conference on Energy and Environment Research, ICEER 2017, 17-20 July 2017, Porto, Portugal

Multiscale modelling of packed bed chemical looping reforming

Arpit Singhal[a, b], Schalk Cloete[c], Rosa Quinta-Ferreira[b] and Shahriar Amini[a,c]*

[a] NTNU: *Norwegian University of Science and Technology, Department of Energy and Process Engineering, NO-7491, Trondheim, Norway*
[b] *University of Coimbra, Department of Chemical Engineering, Rua Sílvio Lima, Polo II, 3030-790 Coimbra, Portugal*
[c] *SINTEF Materials and Chemistry, Flow Technology Department, S. P. Andersens veg 15 B, NO-7031, Trondheim, Norway*

Abstract

A comparison of reactive flows on two distinct scales is presented here (i) Particle resolved direct numerical simulation (PR-DNS), and (ii) 1D packed bed model. The PR-DNS geometry is meshed with polyhedral elements both inside and outside the particle to directly resolve the phenomena of intra particle diffusion and external heat and mass transfer. In contrast, the 1D packed bed model incorporates appropriate closure models to compare against the PR-DNS solutions at a computational cost several magnitudes less. Simulations are performed for endothermic steam methane reforming reactions (SMR) over a range of inlet temperatures. The comparison of the results between the two approaches shows that the 1D model can adequately replicate the PR-DNS results with appropriate modifications to the closures. The resulting verified 1D model was then used to simulate the reforming stage of an industrial scale packed bed chemical looping reforming reactor.

Peer-review under responsibility of the scientific committee of the 4th International Conference on Energy and Environment Research.

Keywords: CFD-DEM; Direct Numerical Simulation (DNS); heat transfer; multiscale; packed bed; reaction rate; steam methane reforming

1. Introduction

Packed bed reactors are extremely relevant to the chemical and process industry, with wide variety of uses in adsorption, heat exchangers, chemical reforming, etc. With the development in the field of computational resources, it is now possible to obtain resolved 3D CFD simulations of flow around arrays of packed particles.

* Corresponding author. Tel.: +4746639721
E-mail address: shahriar.amini@sintef.no

1876-6102
Peer-review under responsibility of the scientific committee of the 4th International Conference on Energy and Environment Research.
10.1016/j.egypro.2017.10.287

PR-DNS can provide insight into the local phenomena of velocities and void fractions in the packed beds, which cannot be obtained from experiments. There have been several attempts to model the intra particle diffusion, but most of studies used the particles as the porous regions [1]. The detailed review of several works done for intra particle diffusion is given by Dixon [2]. Dixon [2] presented the most recent work with 3D CFD simulations for heterogeneous catalytic reactions in a tube packed bed ($3 \leq N \leq 10$), having reactions inside the catalytic particle and not just confined to the exterior surface for steam methane reforming (SMR) endothermic reaction.

The objective of the current work is to evaluate the prediction of endothermic steam methane reforming (SMR) on two distinct scale. Firstly, PR-DNS is used on a geometry of ~100 densely packed mono-disperse spherical particles ($\varepsilon = 0.355$) extracted in a way shown in our previous works [3, 4]. Secondly, computationally affordable 1D packed bed model which is based on appropriate models for effectiveness factor [5] and external heat and mass transfer [6]. The comparison between both the approaches for specie concentration and temperature differences are documented and the verified 1D model is used to an industrial-scale simulation of reforming in a packed bed chemical looping reforming (PBCLR) reactor.

Nomenclature

Greek Symbols		Nu	Nusselt number ($h\ d_p/k_g$)
α	Volume fraction	P	Pressure [Pa]
ε	Void fraction	Pr	Prandtl number ($\mu\ C_p/k_g$)
ϕ	Thiele modulus (Th)	R	Gas constant [8.314 J/mol/K]
η	Effectiveness factor	r	Radius [m]
ρ	Density (kg/m^3)	Re	Reynolds number ($\rho\ u_s\ d_p/\mu$)
Latin Symbols		Sc	Schmidt number ($\mu/\rho\ D$)
a	Characteristic length of spherical particle ($r_p/3$)	T	Temperature [K]
C_p	Specific heat capacity of gas [J/kg·K]	u_s	Superficial velocity of the gas [m/s]
E_a	Activation energy [J/mol]	*Sub/superscripts*	
h_e	effective heat transfer coefficient [W/m^2·K]	g	Gas
k_0	Arrhenius constant [1/s]	p	Particle
kg	Thermal conductivity of gas [W/m·K]		

2. Methodology

2.1. PR-DNS simulation setup

The realistically packed bed of monodisperse spherical particles ($\varepsilon = 0.355$) is generated using discrete element method (DEM) in *ANSYS FLUENT* as explained in detail in our previous works [3, 4].

The SMR reaction takes place inside the porous particles (grain model [7]) according to Eq. (1)-(3). The simulation parameters used are given in Table 1. The reactions were modeled using the kinetic model of Langmuir-Hinshelwood methodology proposed by Xu and Fremont [8] with appropriate kinetic and equilibrium constants from [9].

$$CH_4 + H_2O \leftrightarrow CO + 3H_2 \quad Rx1 \tag{1}$$

$$CO + H_2O \leftrightarrow CO_2 + H_2 \quad Rx2 \tag{2}$$

$$CH_4 + 2H_2O \leftrightarrow CO_2 + 4H_2 \quad Rx3 \tag{3}$$

Simulations are completed for three different values for inlet temperature (Table 1). The molecular diffusivity and gas thermal conductivity are obtained according to the kinetic theory of gases.

Table 1: Simulation parameters for PR-DNS

Parameter	Value	Parameter	Value
Particle diameter (d_p) (m)	0.005	Inlet mole fraction ratio (CH_4:H_20)	1:2
Packed bed voidage	0.355	Specific heat capacity (C_p) (solid) (J/kg/k)	1200
Particle void fraction (internal)	0.3	Thermal conductivity (solid) (W/m.K)	1.0
Density (solid) (kg/m^3)	2500	Operating pressure (bar)	20
Gas velocity (m/s)	0.5	Inlet temperature (°C)	1100,1000, 900

2.2. 1D packed bed model

The 1D model setup used is developed considering 100 cells in one direction with solid phase velocity fixed to zero in all these cells. The model is consistent with the previous works of the authors [4, 10, 11].

The closures [3, 5] represented in Eqns. (4)-(7) are used in conjunction with the same reaction kinetics and boundary conditions as the PR-DNS simulation. The Thiele modulus (ϕ) represents the ratio of kinetic rate to diffusion rate, so higher values represent greater mass transfer limitation. The effective diffusivity (D_e) is composed of the molecular diffusivity (D), the void fraction of porous particles ($\varepsilon = 0.3$) and the tortuosity ($\tau = 1$).

$$Nu = 2.67 + 0.53Re^{0.77}Pr^{0.53} \tag{4}$$

$$\phi = a\sqrt{\frac{k}{D_e}} \tag{5}$$

$$\eta = \frac{1}{\phi}\left(\frac{1}{tanh(3\phi)} - \frac{1}{3\phi}\right) \tag{4}$$

$$D_e = \frac{D\varepsilon}{\tau} \tag{7}$$

In comparison to the previous works [4, 11], three important complications are introduced: multiple reactions, multiple reactants per reaction and the generation of gas volume during the reaction. However, multiple reactions is not so important because the overall steam methane reforming (Rx3) reaction is much faster than the others are.

Gas generation within the particle was found to be the most important effect. Specifically, a convective flux of gas going out of the particle would reduce the rate at which reactants can diffuse into the particle, leading to the effective diffusivity shown below.

$$D_e = \frac{D\varepsilon}{\tau} - u_{gvg}l \tag{8}$$

$$u_{\mathrm{gvg}} = \frac{2(r_1+r_3)}{\alpha_p}\,\frac{RT_p}{P}\,\frac{d_p}{\alpha_p 6} \tag{9}$$

The first term on the right of Eq. (8) is the conventional effective diffusivity used to calculate the Thiele modulus and effectiveness factor as described earlier in Section 2.2. The second term represents the convective transport of species in the opposite direction as the reactant diffusion. The length scale (l) represents the distance covered by the diffusion gradient and should be in the order of the particle radius. The outwards superficial velocity due to gas volume generation $\left(\mathrm{u_{gvg}}\right)$ is estimated at the particle surface according to Eq. (9), where r_1 and r_3 represents the reaction rates for Rx1 and Rx3 respectively. The first term represents the generation of gas inside the particles (mol/m3.s), the second term converts the molar generation rate to a volumetric generation rate via the ideal gas law and the final term (inverse of the surface area per unit volume of monodisperse spheres) converts this volumetric gas generation rate to a velocity at the particle surface (m/s).

For the fast OSMR reaction, inclusion of this effect had a large negative effect on the overall reaction rate by reducing the effective rate of reactant diffusion into the particle, thereby increasing the Thiele modulus and decreasing the effectiveness factor. To account for the effect of multiple reactants, the effectiveness factor was calculated for each reactant species individually and then combined to estimate the overall effectiveness factor: $\eta = (\eta_1^{-1} + \eta_2^{-1})^{-1}$.

The effect of the convective flux out of the particle on the external heat transfer coefficient was estimated in a similar manner. Given that heat diffusion is substantially faster than mass diffusion when a gas is pressurized, this effect was much smaller.

$$h_e = \left(\frac{k_g Nu}{d_p} - u_{gvg}\rho_g C_{p,g}\right)\beta \tag{10}$$

Again, the first term on the right represents the conventional effective heat transfer rate due to heat diffusion through the boundary layer around the particle. The second term represents the convective heat flux in the opposite direction due to the gases exiting the particle at the particle temperature. Experience also showed that the heat transfer rate had to be multiplied by a factor ($\beta < 1$) to match well with PR-DNS results. This implies that the convective flux of gas out of the particle thickens the boundary layer around the particle, adding more heat transfer resistance.

3. Results

3.1. PR-DNS results

Contour plots for methane mole fraction and temperature are shown in Fig. 1. The effects of heat and mass transfer limitations are clearly visible. A gradual species concentration gradient is visible inside the particles (Fig. 1, left) signifying an internal mass transfer limitation. However, the temperature inside the particles is relatively uniform (Fig. 1, right), implying that external heat transfer limitations dominate.

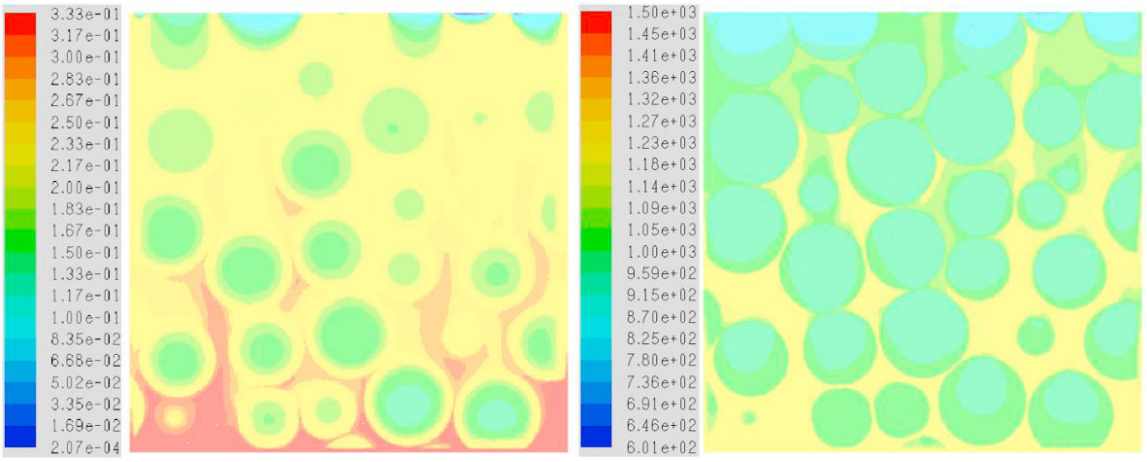

Fig. 1. PR-DNS results for molar concentration of CH_4 (left) and gas temperature (K) variation at 1000 °C inlet temperature.

3.2. Comparison of 1D model to PR-DNS results

Firstly, the 1D model was run without accounting for the outwards velocity resulting from the gas volume generation due to reaction. The resulting comparisons of species and concentration profiles are given in Fig. 2. Some clear deviations between the 1D and PR-DNS results are evident.

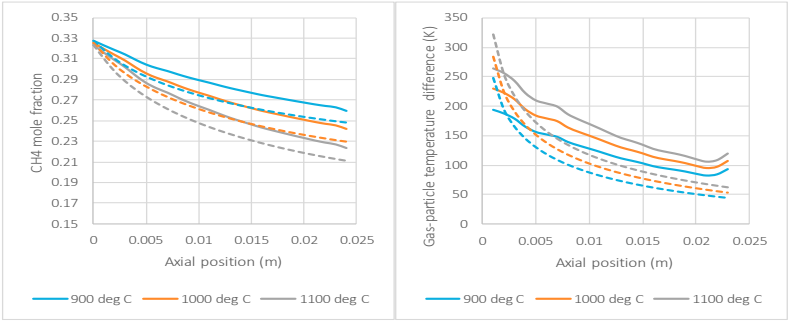

Fig. 2. Axial profiles of methane mole fraction (left) and temperature difference between gas and particles (right) when the gas generation effect is ignored.

The over predicted reaction rate is particularly evident towards the start of the reactor where the 1D model predicts a faster decline in methane concentration than the PR-DNS. This faster endothermic reaction is also reflected in the slight over prediction of gas-particle temperature difference due to the large amount of heat consumption inside the particles where the reaction takes place. Towards the middle of the geometry, however, the reaction rates between the two models are similar, but the temperature difference predicted by the 1D model is much smaller. This suggests an over prediction of the external heat transfer.

Subsequently, the effects of the generated gas were included in the 1D model. Trial and error experimentation showed that a very good match could be attained if the species diffusion length scale (l in Eq. (8)) is set to 1.8 mm and the external heat transfer modification (β in Eq. (9)) is set to 0.7. This good match is shown in Fig. 3.

The main effect of the inclusion of the outwards velocity in Eq. (8) is a large reduction in the effective reaction rate near the reactor inlet. At the start of the domain, the OSMR and SMR reactions are far from equilibrium and the temperature is still high, implying a very fast reaction rate. However, a faster reaction rate from these reactions causes more gas formation inside the particle and thus a larger convective flux out of the particle, counteracting reactant diffusion into the particle. For the OSMR reaction, this effect halved the reaction rate near the inlet.

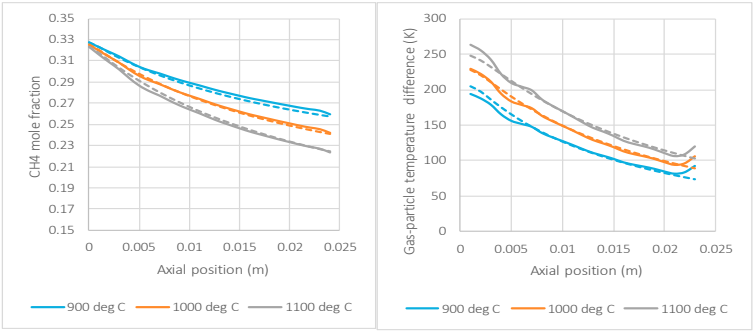

Fig. 3. Axial profiles of methane mole fraction (left) and temperature difference between gas and particles (right) when the full modifications in Eqns. (8), (9) and (10) are implemented.

3.3. The reforming stage of the PBCLR process

The verified model from the previous section was then used to simulate the reforming stage of a large-scale packed bed chemical looping reforming (PBCLR) reactor (10 m in length). The PBCLR process completes an oxidation and reduction stage in a similar way as in the packed bed chemical looping combustion concept [10, 12],

but then uses the heat stored in the bed to complete a long reforming stage instead of a heat removal stage for power production.

The reforming stage of the PBCLR process will take place after the bed has been oxidized by air and reduced by fuel. At that point, the bed is fully reduced and a lot of heat is stored in the oxygen carrier to sustain the endothermic reforming reaction.

In this case, it was assumed that the whole bed is at 1000 °C at the start of the reforming stage. Fig. 4 shows outputs from the simulation where gas was fed with a 1:2 CH_4:H_2O ratio at 300 °C.

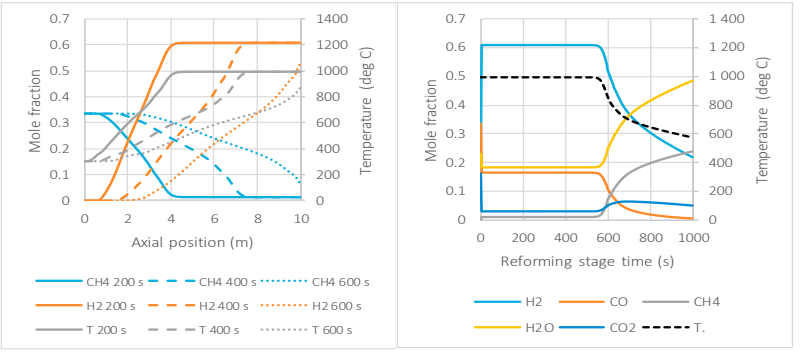

Fig. 4. Axial species and temperature profiles along the bed at different times (left) and outlet species and temperature profiles during the reforming stage of the PBCLR process (right).

The PBCLR process works in a similar manner as the gas switching reforming (GSR) [13, 14] process that utilizes a fluidized bed instead of a packed bed. An attractive feature of the PBCLR reactor over the GSR reactor is that the outlet concentrations and temperature remains constant for a long time during the reforming stage (nearly up to 600 s in Fig. 4), whereas the conversion will decline gradually from the start of the reduction stage in the GSR concept as the bed cools down. This is a result of the plug-flow nature of the PBCLR concept. In practice, this will allow the PBCLR process to be operated at lower temperatures or higher pressures, while achieving similar performance to the GSR concept.

4. Conclusion

This work presented a comparison of particle resolved direct numerical simulation (PR-DNS) with 1D packed bed model for a densely packed bed on mono disperse spherical particles in a reacting system of steam methane reforming. The 1D model along with recently proposed closure models for external heat and mass transfer using modification factors to account for the deviation caused by over prediction of particle temperature in 1D model approximates well with the PR-DNS results. Verified models used to simulate a reforming stage of a large scale packed bed chemical looping reforming (PBCLR) suggests promising results with the PBCLR processes.

Acknowledgements

This work is a part of a European Union project under Seventh research framework program (FP7/2007-2013) under grant agreement n° 604656 - (NanoSim). The authors are grateful to European Research Council for its support. The computational resources at NTNU provided by NOTUR, http://www.notur.no, were used during this project.

References

[1] Karthik GM, Buwa VV, Effect of particle shape on fluid flow and heat transfer for methane steam reforming reactions in a packed bed, AIChE Journal 2017;63:366-377.

[2] Dixon AG, Local transport and reaction rates in a fixed bed reactor tube: Endothermic steam methane reforming, Chemical Engineering Science 2017;168:156-177.
[3] Singhal A, Cloete S, Radl S, Quinta-Ferreira R, Amini S, Heat transfer to a gas from densely packed beds of monodisperse spherical particles, Chemical Engineering Journal 2017;314:27-37.
[4] Singhal A, Cloete S, Radl S, Quinta-Ferreira R, Amini S, Comparison of Particle-Resolved Direct Numerical Simulation and 1D modelling of catalytic reactions in a packed bed, In: 12th International Conference on CFD in Oil & Gas, Metallurgical and Process Industries, SINTEF, Trondheim, Norway. 2017, pp. 667-674.
[5] Levenspiel O. Chemical Reaction Engineering, 3rd ed, John Wiley & Sons, New York.; 1999.
[6] Gunn DJ, Transfer of heat or mass to particles in fixed and fluidised beds, International Journal of Heat and Mass Transfer 1978;21:467-476.
[7] Szekely J, Evans, J.W., Sohn, H.Y.,. Gas-solid reactions, Academic Press, New York; 1976.
[8] Xu J, Froment GF, Methane steam reforming, methanation and water-gas shift: I. Intrinsic kinetics, AIChE Journal 1989;35:88-96.
[9] Oliveira ELG, Grande CA, Rodrigues AE, Methane steam reforming in large pore catalyst, Chemical Engineering Science 2010;65:1539-1550.
[10] Cloete S, Gallucci F, van Sint Annaland M, Amini S, Gas Switching as a Practical Alternative for Scaleup of Chemical Looping Combustion, Energy Technology 2016;4:1286-1298.
[11] Singhal A, Cloete S, Quinta-Ferreira R, Amini S, Comparison Of Particle-Resolved Direct Numerical Simulation And 1d Modelling Of Catalytic Reactions In A Cylindrical Particle Bed, In: V International Conference on Particle-based Methods. Fundamentals and Applications (Eccomas Thematic Conference), CIMNE, Hannover, Germany. 2017.
[12] Noorman S, van Sint Annaland M, Kuipers, Packed Bed Reactor Technology for Chemical-Looping Combustion, Industrial & Engineering Chemistry Research 2007;46:4212-4220.
[13] Wassie SA, Gallucci F, Zaabout A, Cloete S, Amini S, van Sint Annaland M, Hydrogen production with integrated CO2 capture in a novel gas switching reforming reactor: Proof-of-concept, International Journal of Hydrogen Energy 2017;42:14367-14379.
[14] Francisco Morgado J, Cloete S, Morud J, Gurker T, Amini S, Modelling study of two chemical looping reforming reactor configurations: looping vs. switching, Powder Technology 2016.